Electronic Supplementary Material (ESI) for Journal of Materials Chemistry A

Supporting Information

A Highly Active and Stable Electrocatalyst for Oxygen Reduction Reaction Based on Graphene Supported g-C_3N_4@Cobalt Oxide Core-Shell Hybrid

Jutao Jin,[a, b] Xiaogang Fu,[a,c] Qiao Liu[a,b] and Junyan Zhang[a,*]

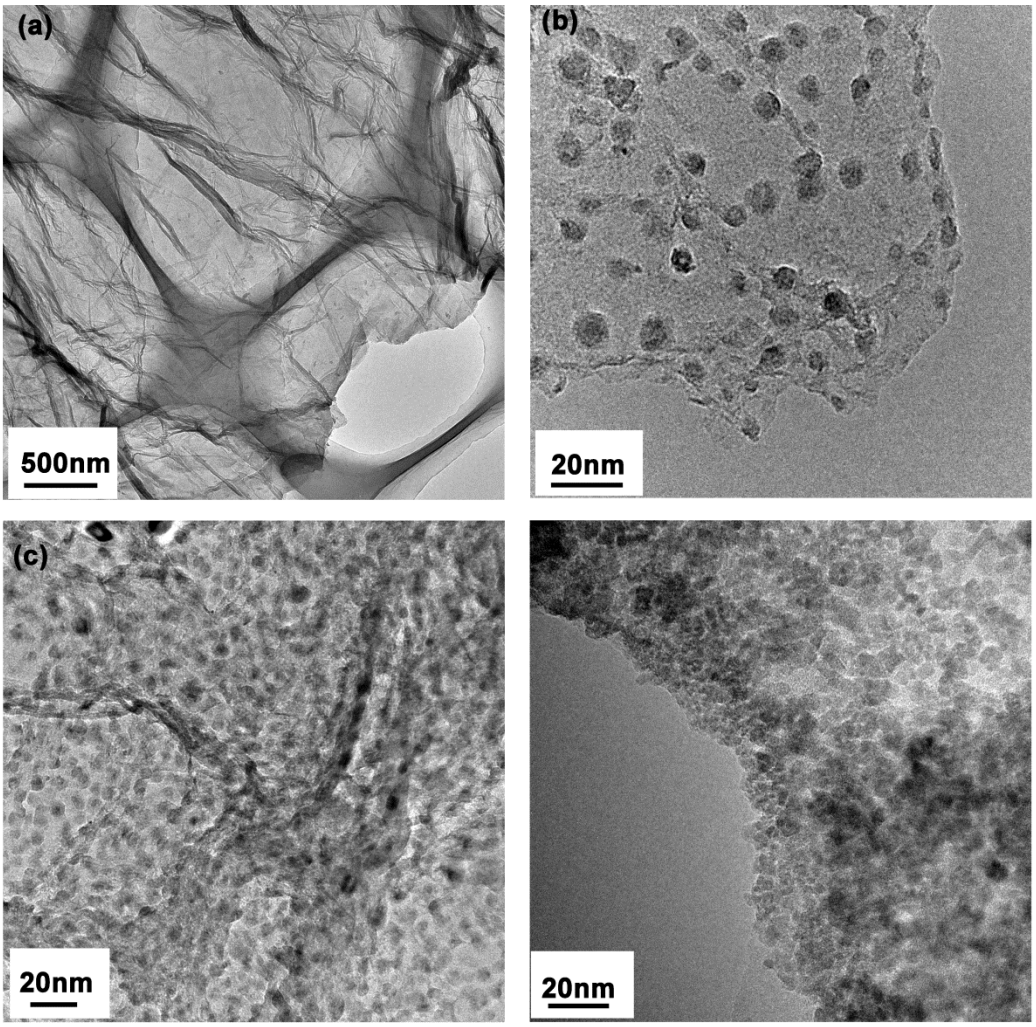

Figure S1. TEM images of (a) g-C_3N_4/GS hybrid (b) NCo-GS-0.25 hybrid (c) NCo-GS-0.5 hybrid (d) NCo-GS-1 hybrid.

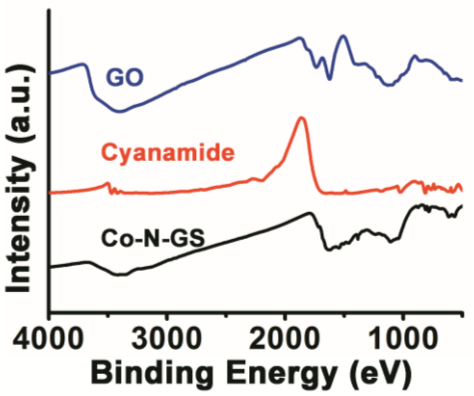

Fig S2 FTIR patterns of Co-N-GS and GO and Cyanamide.

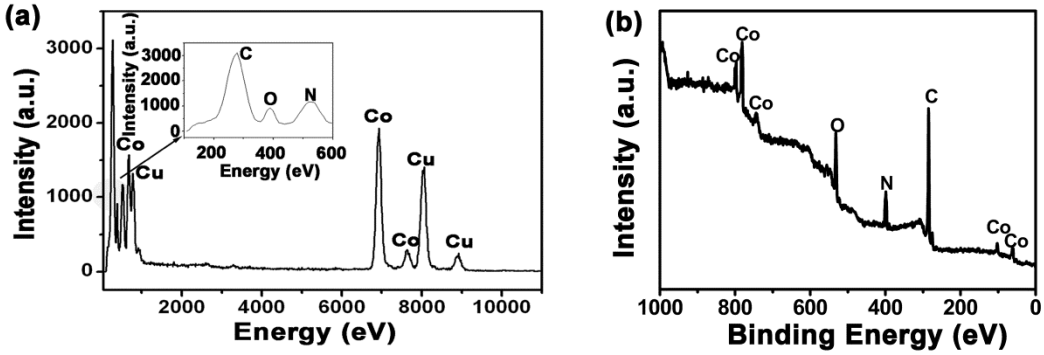

Figure S3. (a) EDS spectra of the NCo-GS-0.5 hybrid, inset shows the high resolution spectrum of C, N, O at low energy range; (b) XPS spectrum of Nco-GS-0.5 hybrid.

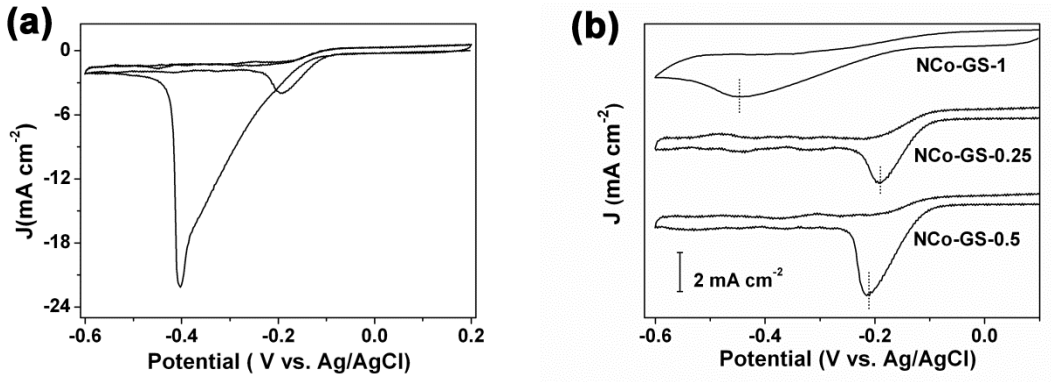

Figure S4. (a) The first two cycles of CV curve of NCo-GS-0.5 hybrid electrode in O_2-saturated 0.1M KOH at a scan rate of 50mV s^{-1}. (b) CV curves of NCo-GS-0.25 hybrid, NCo-

GS-0. 5 and NCo-GS-1 hybrid loaded on glass carbon electrode in O_2-saturated 0.1M KOH at a scan rate of 50mV s^{-1}.

The first two voltammograms (CV) cycles of NCo-GS-0.5 in O_2-saturated 0.1 M KOH solutions at a scan rate of 50 mV s^{-1} display two reduction current peaks, with a big one centered at -0.41V and a small one centered at -0.22V, corresponding to the first and second CV cycle, respectively(Figure S4a). The reduction peak at lower potential is quite asymmetrical, suggesting that the reduction species are not from electrolyte solution (commonly display a symmetrical diffusing reduction peak) but from surface-confined species adsorbed at the surface of the catalyst.[S2]The large reduction peak indicates rich adsorbed oxygen species at the catalyst surface which was previously confirmed by XPS results (Figure S3a). The smaller reduction peak at -0.21V is a typical diffusion controlled reduction peak.

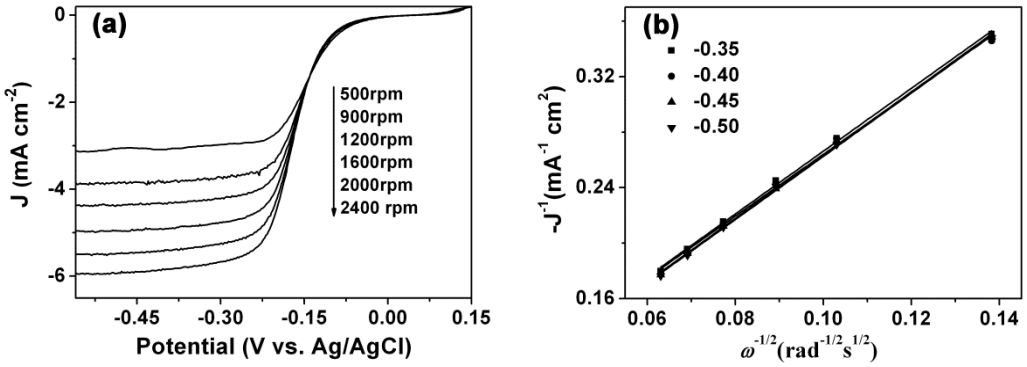

Figure S5. (a) Rotating-disk voltammograms of NCo-GS-0.5 hybrid in O_2-saturated 0.1M KOH at a scan rate of 5mV s^{-1} at different rotation rates and the corresponding (b) Koutecky–Levich plot of J^{-1} versus □$^{-1/2}$. (c) Rotating-disk voltammograms of NCo-GS-0.5 hybrid in O_2-saturated 0.1M KCl at a scan rate of 5mV s^{-1} at different rotation rates and the corresponding (d) Koutecky–Levich plot of J^{-1} versus □$^{-1/2}$.

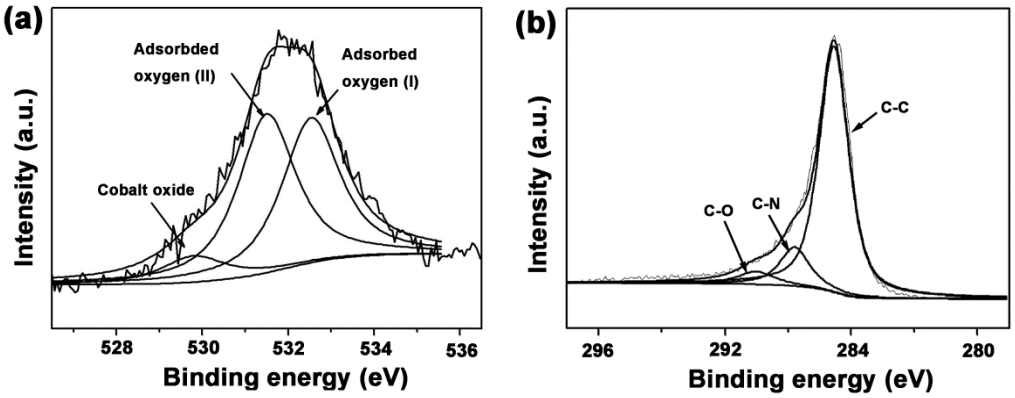

Figure S6 . High resolution XPS spectra of O1s (a) and C1s (b) of NCo-GS-0.5 hybrid.

The O1s and C1s high resolution XPS spectra of NCS-GS-0.5 hybrid are shown in Figure S1a and Figure S1b, respectively. The C1s bond can be deconvoluted into three bands at 284.6eV, 285.9eV and 287.2eV, which can be assigned to C=C, C-N (C=N) and C-O(C=O), respectively. The O1s bond can be deconvoluted into three bands at 529.8eV and 531.5eV and 532.3eV. According to the literature,[S1] the binding energy at 529.8eV belongs to the lattice oxide oxygen in cobalt oxide. The two subpeaks at 531.5 and 532.3 belong to the surface adsorbed oxygen species. The adsorbed oxygen (I) and adsorbed oxygen(II) labelled in Figure S3a. can be assigned to oxygen adsorbed on CoN_2 and CoN_6 site, respectively.

Table S1. Elemental composition of as-prepared NCo-GS

Samples	Analysis Method	Carbon (at.%)	Nitrogen (at.%)	Oxygen (at.%)	Cobalt (at.%)
NCo-GS-0.25	EDS[a]	80.16±1.56	7.03±0.34	8.23±0.29	4.58±0.11
	XPS	72.69±2.03	8.37±0.23	12.48±0.15	6.46±0.11
NCo-GS-0.5	EDS	75.33±1.98	8.12±0.88	9.67±0.47	6.78±0.41
	XPS	65.46±2.56	9.15±1.22	16.73±1.46	8.46±0.32
NCo-GS-1	EDS	60.38±1.38	8.99±0.84	18.46±1.17	12.17±0.89
	XPS	55.16±1.59	11.12±0.97	19.47±2.22	14.25±0.98
Co-N-GS	EDS	75.72±2.31	8.77±0.79	9.18±0.86	6.33±0.47
	XPS	72.20±1.98	9.01±0.67	11.22±0.83	7.57±0.35

[a]:Cu element was deducted for EDS analysis

Table S2. Comparison of catalytic activity data of recent report g-C_3N_4 /carbon hybrid as ORR electrocatalyst in basic solution

sample	Half wave potential compared with Pt/C ($\Delta E_{½}$)	kinetic-limiting current density (J_k)	Electron transfer number(n)
g-C_3N_4/graphene [S3]	**100mV**	**-**	**2.5 @ -0.6V (Vs. SCE)**
g-C3N4@CMK-3[S4]	**50mV**	**11.3 mA cm^{-2} at -0.5V (Vs. Ag/AgCl)**	**4 @ -0.6V (Vs.Ag/AgCl)**
macroporous g-C_3N_4/Carbon[S5]	**55mV**	**-**	**3 @-0.6V (Vs.Ag/AgCl)**
This work	**25mV**	**16.78 mA cm^{-2} at -0.25V (Vs. Ag/AgCl)**	**3.7 @-0.6V (Vs. Ag/AgCl)**

S1. a) J.-C. Dupin, D. Gonbeau, P. Vinatier, A. Levasseur, Phys. Chem. Chem. Phys. 2000, 2, 1319. b) J. Long, X. Xie, J. Xu, Q. Gu, L. Chen, X. Wang, *ACS Catal.* 2012, 2, 622.

S2. J. Chlistunoff, *J. Phys. Chem. C.* 2011, 115, 6496.

S3. Y. Sun, C. Li, Y. Xu, H. Bai, Z. Yao, G. Shi, *Chem. Commun.* **2010**, *46*, 4740-4742.

S4. Y. Zheng, Y. Jiao, J. Chen, J. Liu, J. Liang, A. Du, W. Zhang, Z. Zhu, S. C. Smith, M. Jaroniec, G. Q. Lu, S. Z. Qiao, *J. Am. Chem. Soc.* **2011**, *133*, 20116-20119.

S5. J. Liang, Y. Zheng, J. Chen, J. Liu, D. Hulicova-Jurcakova, M. Jaroniec, S. Z. Qiao, *Angew. Chem.* **2012**, *124*, 3958-3962; *Angew. Chem., Int. Ed.***2012**, *51*, 3892-3896;